ChemComm

COMMUNICATION

View Article Online
View Journal | View Issue

Cite this: *Chem. Commun.*, 2025, **61**, 17388

Received 3rd September 2025,
Accepted 6th October 2025

DOI: 10.1039/d5cc05091j

rsc.li/chemcomm

A multicomponent approach for the stereoselective synthesis of atropisomeric N–N peptide analogues

Natalie J. Roper, [a] George M. Hardy, [a] Jack M. Wootton, [a] Paul G. Waddell, [a] James Wilson[b] and Roly J. Armstrong *[a]

Peptide analogues featuring both central and N–N axial chirality were efficiently synthesised using a 4-component Ugi reaction. This method demonstrates a broad substrate scope, affording the target compounds with excellent stereoselectivity (up to >95 : 5 d.r.). Thermal atropisomerization studies revealed the identity of the substituents significantly influences the configurational stability and thermodynamic preferences of the atropisomeric products.

Atropisomers are valuable chiral molecules whose stereogenicity arises *via* restricted rotation about a single bond. To date, most studies in this area have explored systems whose chirality is derived from restricted C–C or C–N bond rotation,[1] but recently atropisomeric compounds featuring a stereogenic N–N axis have gained prominence as valuable bioactive scaffolds (Scheme 1A).[2] For example, the N–N atropisomeric natural product Schischkiniin exhibits activity against Caco-2 colon cancer cell lines,[3] and the indolosesquiterpene alkaloid dixiamycin A is active against several strains of bacteria.[4] N–N atropisomerism is also a key structural element in non-natural bioactive small molecules, for example bispyrroles reported by Zhang, Shi and co-workers, displaying promising activity against QGP-1 cancer cells.[5] The emerging utility of these scaffolds has inspired the development of various powerful strategies for the synthesis of N–N atropisomers, including *N*-functionalization, *de novo* ring formation, C–H functionalization and desymmetrization approaches.[6]

Despite these advances, the integration of N–N atropisomerism into peptidomimetics (molecules designed to mimic the structure and function of peptides) remains markedly underexplored. A pioneering contribution in this area was reported by Gütschow and co-workers, who showed that bis-methylated azadipeptides could be prepared *via* *N*-acylation (Scheme 1B).[7] These scaffolds were shown to display class 2 atropisomerism, with free energy barriers for enantiomerization ($\Delta G^{\ddagger}$) up to 117 kJ mol^{-1}. Substituted α-amino acids ($R^1 \neq H$) could be introduced, leading to the formation of diastereoisomeric mixtures of products. Very recently, Proulx and co-workers explored the late-stage alkylation of more complex azapeptides, affording class 1–2 atropisomeric dialkylated azapeptides ($\Delta G^{\ddagger}$ = 63–100 kJ mol^{-1}).[8] Proulx and co-workers have also reported evidence of atropisomerism within metallo-azapeptides, where co-ordination of the hydrazide nitrogen to a palladium centre imparts restricted N–N rotation.[9] Despite these important advances, the synthesis of N–N atropisomeric peptide frameworks remains significantly underdeveloped. In particular, no general methods are available to access configurationally robust class 3 atropisomeric N–N atropisomeric peptide analogues, or to achieve kinetic control over their relative stereochemistry.[10] With these challenges in mind, based upon our

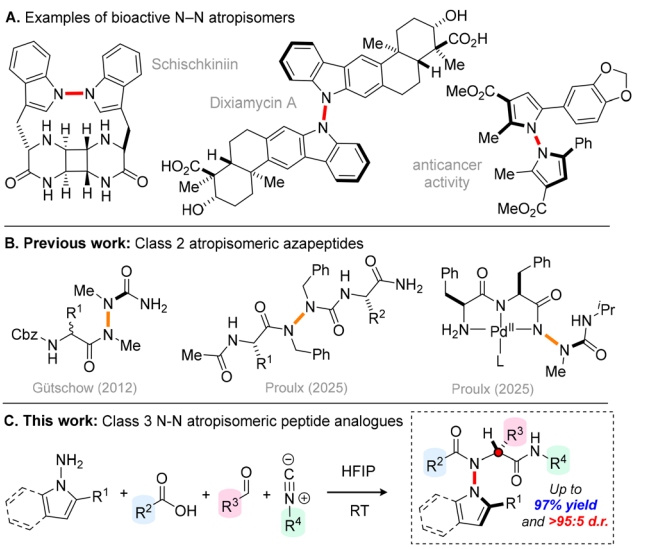

Scheme 1 Previous work and strategy for the synthesis of N–N atropisomeric peptide analogues.

[a] *Chemistry – School of Natural and Environmental Sciences, Newcastle University, Newcastle Upon Tyne, NE1 7RU, UK. E-mail: roly.armstrong@newcastle.ac.uk*
[b] *Chemical Development, Pharmaceutical Technology and Development, AstraZeneca, Macclesfield Campus, Macclesfield, SK10 2NA, UK*

recent work on C–N atropisomeric scaffolds, we envisioned that it might be possible to prepare N–N atropisomeric peptide analogues *via* a four-component Ugi reaction between sterically encumbered *N*-aminated heterocycles, aldehydes, carboxylic acids and isocyanides (Scheme 1C).[10a] Based upon previous reports, we believed that these products would display stable atropisomerism and the proposed methodology could provide an efficient and modular approach for their diastereocontrolled synthesis.[6] Herein, we report the successful realization of this goal, with a library of 22 N–N atropisomeric peptide analogues prepared in up to 97% yield and >95 : 5 d.r. Kinetic epimerization studies reveal these scaffolds to be configurationally robust class 3 atropisomers, with $\Delta G^{\ddagger}$ = 132–144 kJ mol^{-1}, with the substitution pattern playing a key role in dictating the rate and position of equilibrium in the atropisomerization process.

We commenced our study by exploring a model multicomponent reaction between methyl 1-amino-1*H*-indole-2-carboxylate (**1a**), benzaldehyde (**2a**), benzoic acid (**3a**), and *tert*-butyl isocyanide (**4a**) in 2,2,2-trifluoroethanol (TFE) at room temperature for 24 hours. Pleasingly, the intended Ugi product **5a** was obtained in a modest, but promising 17% yield, and analysis of the crude reaction mixture confirmed that the reaction proceeds with excellent diastereocontrol (>95 : 5 d.r.) (Table 1, entry 1). The relative configuration of the product was unambiguously confirmed using single crystal X-ray analysis, revealing the ester group of the indole and the α-phenyl substituent to have an *anti*-arrangement. Encouraged by this result, we focused on optimising the reaction conditions. Upon replacing the solvent with 1,1,1,3,3,3-hexafluoroisopropanol (HFIP), a substantial increase in yield to 69% was observed (Table 1, entry 2). Furthermore, employing an excess of the isocyanide (2.0 equivalents) led to a further improvement, with the desired product obtained in 79% yield and >95 : 5 d.r. (Table 1, entry 3). We then explored whether addition of a desiccant might improve the efficiency of the transformation by promoting imine formation. While 4 Å molecular sieves produced inferior results, both 5 Å and 3 Å molecular sieves led to slightly increased yields of 80% and 82%, respectively (Table 1, entries 4–6). Finally, we turned our attention back to reagent stoichiometry. Limiting the amount of aldehyde **2a** in the reaction resulted in a slightly decreased yield (Table 1, entry 7). In contrast, employing aminated indole **1a** as the limiting reagent led to a significant increase in conversion, enabling the isolation of the product **5a** by column chromatography in 89% yield as a single diastereoisomer (Table 1, entry 8). The selectivity for the *anti*-diastereoisomer was confirmed *via* a thermal epimerization experiment, which enabled unambiguous characterization of *syn*-**5a** (*vide infra*).

Table 1 Optimization of diastereoselective 4-component coupling. Reaction Conditions: rt, 24 h

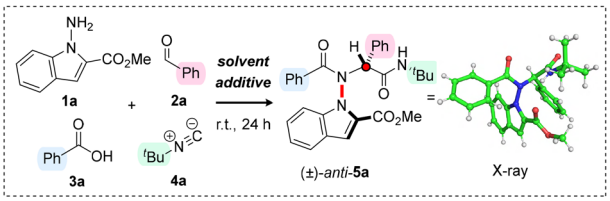

Entry	Solvent (0.5 M)	1a : 2a : 3a : 4a	Additive	Yield *anti*-5a (%)[a]	d.r. *anti*-5a[b]
1	TFE	1 : 1 : 1 : 1	—	17	>95 : 5
2	HFIP	1 : 1 : 1 : 1	—	69	>95 : 5
3	HFIP	1 : 1 : 1 : 2	—	79	>95 : 5
4	HFIP	1 : 1 : 1 : 2	4 Å MS	76	>95 : 5
5	HFIP	1 : 1 : 1 : 2	5 Å MS	80	>95 : 5
6	HFIP	1 : 1 : 1 : 2	3 Å MS	82	>95 : 5
7	HFIP	1.2 : 1 : 1.2 : 2	3 Å MS	81	>95 : 5
8	HFIP	1 : 1.2 : 1.2 : 2	3 Å MS	87 (89)	>95 : 5

[a] Yields determined by quantitative ^{1}H NMR analysis *vs.* $(CH_3)_2SO_2$ as an internal standard; values in parentheses indicate the yield of isolated product. [b] Diastereoselectivity determined by ^{1}H NMR analysis of the crude reaction mixture.

With optimal conditions in hand, we next investigated the generality of the reaction (Scheme 2). A range of aromatic aldehydes, including examples bearing unprotected phenols (*anti*-**5b**) and sterically demanding groups (*anti*-**5c–5e**), afforded the corresponding products in high yields and excellent diastereoselectivity (>95 : 5 d.r.). Encouragingly, the methodology also proved effective with aliphatic aldehydes, with products *anti*-**5f–5h** isolated in similarly high yields and stereoselectivity. We next explored the scope of the carboxylic acid partner. Electron-rich benzoic acid analogues were well tolerated, furnishing products *anti*-**5i** and *anti*-**5j** in reasonable yields and high diastereomeric ratios (>95 : 5 and 94 : 6 d.r. respectively). Electron-deficient and heteroaromatic carboxylic acids were also effective substrates, delivering atropisomeric products *anti*-**5k–5l** with good stereoselectivity (92 : 8 d.r.). Aliphatic carboxylic acids also underwent the desired multicomponent reaction, enabling access to peptide analogues *anti*-**5m–5o** in good yields albeit with slightly diminished diastereoselectivities (80 : 20–88 : 12 d.r.). Collectively, these results demonstrate the steric and electronic properties of the acid component significantly influence the stereochemical outcome of the reaction. A selection of commercially available isocyanides were examined, which all reacted smoothly under the reaction conditions, delivering compounds *anti*-**5p–5r** with essentially complete diastereocontrol (>95 : 5 d.r.). Finally, we explored the scope of the heterocyclic locking group. Aminated indoles bearing different backbone substituents reacted efficiently, affording the corresponding products *anti*-**5s–5t** in moderate to good yields and excellent diastereoselectivity (>95 : 5 d.r.). The ester substituent could also be varied with an isopropyl analogue *anti*-**5u** obtained in 67% yield and >95 : 5 d.r. Finally, we found that 2,5-disubstituted aminated pyrroles could also be successfully employed in the reaction, yielding atropisomeric peptide *anti*-**5v** with similarly high stereoselectivity (94 : 6 d.r.).

To assess the configurational stability of our N–N atropisomeric peptide analogues, we explored thermal epimerization about the stereogenic axis.[11] Model substrate *anti*-**5a** was heated to 120 °C in DMSO-d_6 for several days, with aliquots removed at regular intervals and analysed by ^{1}H NMR spectroscopy (Scheme 3, gray dataset). Under these conditions, we were pleased to observe smooth epimerization to *syn*-**5a** which was formed in 88 : 12 d.r. with equilibrium achieved after

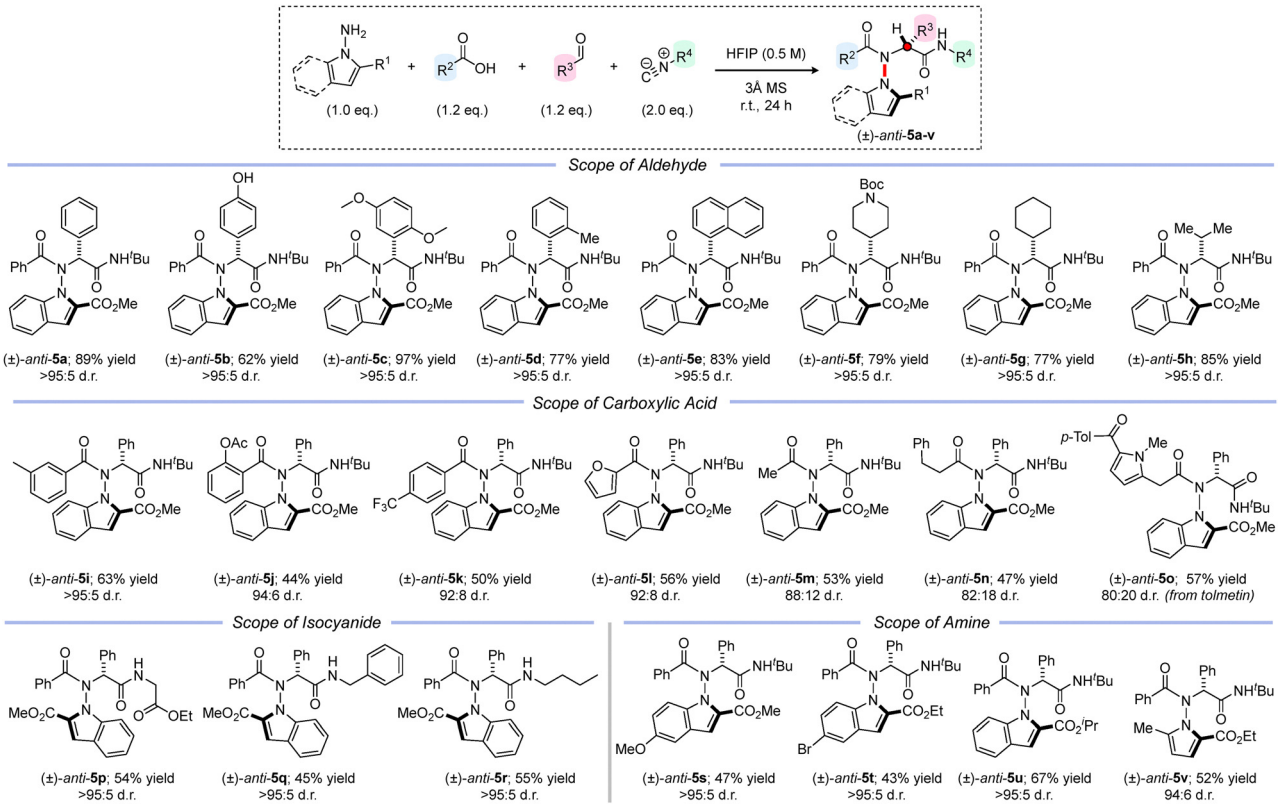

Scheme 2 Stereoselective multicomponent synthesis of N–N atropisomeric amides. Reaction conditions: aminated heterocycle (1.0 equiv.), aldehyde (1.2 equiv.), carboxylic acid (1.2 equiv.), isocyanide (2.0 equiv.), 3 Å molecular sieves (100 mg mL^{-1} solvent), HFIP (0.5 M), r.t., 24 h. Yields refer to isolated material after column chromatography. Diastereoselectivity determined by ^{1}H NMR analysis of the crude reaction mixture.

approximately 60 hours. Note that the structure and relative stereochemistry of *syn*-**5a** were unambiguously confirmed by single crystal X-ray analysis. From the kinetic profile shown in Scheme 3, values for $\Delta G^{\ddagger}$ of 132 kJ mol^{-1} and 139 kJ mol^{-1} for the respective forward and backward isomerization processes of *anti*-**5a** were calculated (see SI for details), confirming class 3 atropisomerism. Furthermore, based upon the final equilibrium ratio of 88 : 12 d.r. we calculated a standard Gibbs free energy difference (ΔG°) between the diastereomers of **5a** of −6.4 kJ mol^{-1}, indicating a clear thermodynamic preference for the *syn*-isomer, which is in line with our previous work on structurally related C–N atropisomeric peptide analogues.[10a]

To explore how the steric and electronic properties of different substituents may influence the stability of these N–N atropisomeric peptide analogues, an analogous epimerization study was performed with *anti*-**5h**, which bears an isopropyl group α- to the carbonyl of the secondary amide (Scheme 3, pink dataset). In this case, isomerization proceeded at a similar rate ($\Delta G_{\text{forward}}^{\ddagger}$ = 134 kJ mol^{-1}; $\Delta G_{\text{backward}}^{\ddagger}$ = 135 kJ mol^{-1}), but intriguingly an almost equimolar ratio of *anti*- and *syn*-**5h** was obtained at equilibrium (ΔG° = −0.4 kJ mol^{-1}). This result indicates that replacing the α-substituent with an aliphatic group preserves class 3 atropisomerism, but effectively eliminates the thermodynamic preference for the *syn*-diastereoisomer. Finally, we investigated the isomerization of *anti*-**5n**, which bears an aliphatic acyl substituent (Scheme 3, blue dataset). Interestingly, in this case epimerization proceeded very slowly when heated to 120 °C, indicating significantly increased configurational stability. Therefore, an additional thermal isomerization experiment was conducted at 150 °C, under which conditions the system reached an equilibrium ratio of 80 : 20 (ΔG° = −4.9 kJ mol^{-1}), which is similar to that of *anti*-**5a**. Based upon this data we calculated values of $\Delta G^{\ddagger}$ of 144 kJ mol^{-1} and 148 kJ mol^{-1} for the respective forward and backward isomerization processes, confirming very high configurational stability.

Taken together, these results may imply that the α-substituent predominantly dictates thermodynamic stability, whereas the acyl substituent impacts the kinetics of epimerization. The substantially slower rate of isomerization for examples bearing an aliphatic acyl substituent is in line with our previous work on C–N atropisomeric amides, which was attributed to a racemization mechanism involving correlated bond rotation.[12] We tentatively conclude that a similar mechanism involving geared rotation of the N–N and N–CO bonds may also be operative in N–N atropisomeric amides.

In summary, we have developed an efficient multicomponent approach for the synthesis of novel N–N atropoisomeric peptide analogues which proceeds in excellent yields (up to 97%) with very high levels of kinetic selectivity in favour of the *anti*-configured diastereomer (up to >95 : 5 d.r.). Thermal isomerization studies reveal that these molecules are configurationally stable class 3 atropisomers ($\Delta G^{\ddagger} \geq$ 132 kJ mol^{-1}). The thermodynamics and kinetics of the epimerization process appear to be substantially influenced by the α- and acyl

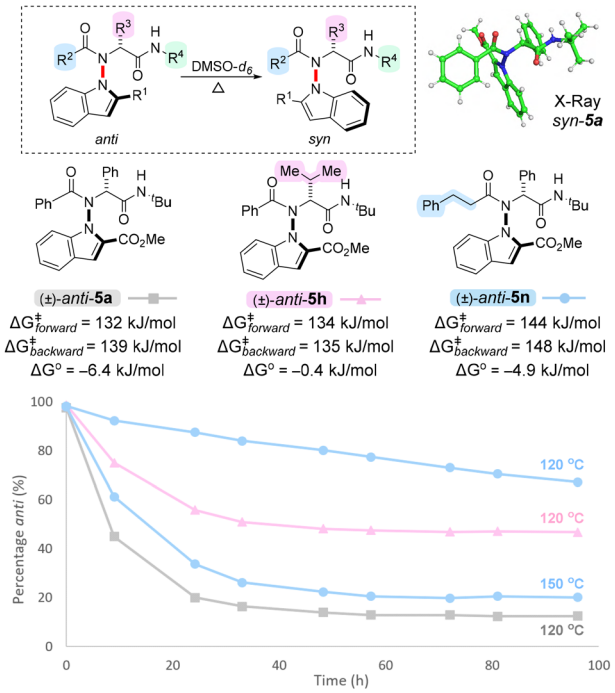

Scheme 3 Thermal isomerization of N–N atropisomeric peptide analogues. Aliquots were removed at regular time intervals with d.r. determined by quantitative ^{1}H NMR analysis (see SI for details).

substituents respectively, and further work is underway in our laboratory to explore the generality of these observations and to assess their implications regarding the mechanism of N–N atropisomerization.

We gratefully acknowledge financial support from EPSRC (EP/S022791/1, UKRI124 and EP/W524700/1) and Newcastle University. N. J. R. thanks the Bill and Milica Beck PhD Endowment Fund. G. M. H. gratefully acknowledges AstraZeneca for studentship support. We are grateful to Dr Corinne Wills and Dr Casey Dixon (Newcastle University) for assistance with NMR experiments.

Conflicts of interest

There are no conflicts to declare.

Data availability

The data underlying this study are available in the published article and in the supplementary information (SI). Supplementary information: detailed experimental procedures and characterization data for new compounds. See DOI: **https://doi.org/10.1039/d5cc05091j**.

CCDC 2476444 and 2476445 contain the supplementary crystallographic data for this paper.[13a,b]

Notes and references

1 For selected review articles, see: (*a*) T. A. Schmidt, V. Hutskalova and C. Sparr, *Nat. Rev. Chem.*, 2024, **8**, 497–517; (*b*) S.-H. Xiang, W.-Y. Ding, Y.-B. Wang and B. Tan, *Nat. Catal.*, 2024, **7**, 483–498; (*c*) J. S. Sweet and P. C. Knipe, *Synthesis*, 2022, 2119–2132; (*d*) Y.-J. Wu, G. Liao and B.-F. Shi, *Green Synth. Catal.*, 2022, **3**, 117–136; (*e*) P. Rodríguez-Salamanca, R. Fernández, V. Hornillos and J. M. Lassaletta, *Chem. – Eur. J.*, 2022, **28**, e202104442; (*f*) A. D. G. Campbell and R. J. Armstrong, *Synthesis*, 2023, 2427–2438.

2 Z. Wang, L. Meng, X. Liu, L. Zhang, Z. Yu and G. Wu, *Eur. J. Med. Chem.*, 2022, **243**, 114700.

3 M. Shoeb, S. Celik, M. Jaspars, Y. Kumarasamy, S. M. MacManus, L. Nahar, P. K. Thoo-Lin and S. D. Sarker, *Tetrahedron*, 2005, **61**, 9001–9006.

4 Q. Zhang, A. Mándi, S. Li, Y. Chen, W. Zhang, X. Tian, H. Zhang, H. Li, W. Zhang, S. Zhang, J. Ju, T. Kurtán and C. Zhang, *Eur. J. Org. Chem.*, 2012, 5256–5262.

5 K.-W. Chen, Z.-H. Chen, S. Yang, S.-F. Wu, Y.-C. Zhang and F. Shi, *Angew. Chem., Int. Ed.*, 2022, **61**, e202116829.

6 For selected review articles, see: (*a*) G. Centonze, C. Portolani, P. Righi and G. Bencivenni, *Angew. Chem., Int. Ed.*, 2023, **62**, e202303966; (*b*) G.-J. Mei, W. L. Koay, C.-Y. Guan and Y. Lu, *Chem*, 2022, **8**, 1855–1893; (*c*) H.-H. Zhang and F. Shi, *Acc. Chem. Res.*, 2022, **55**, 2562–2580; (*d*) J. Feng, C.-J. Lu and R.-R. Liu, *Acc. Chem. Res.*, 2023, **56**, 2537–2554; (*e*) J. Feng and R.-R. Liu, *Chem. – Eur. J.*, 2024, **30**, e202303165.

7 (*a*) P. A. Ottersbach, G. Schnakenburg and M. Gütschow, *Chem. Commun.*, 2012, **48**, 5772–5774; (*b*) P. A. Ottersbach, G. Schnakenburg and M. Gütschow, *Tetrahedron Lett.*, 2015, **56**, 4889–4891.

8 M. E. Helton, C. S. Howard, K. Prieto Bruno, K. D. Cartrette, M. O. Bowles, W. A. Hearne and C. Proulx, *J. Org. Chem.*, 2025, **90**, 9549–9558.

9 M. O. Bowles, E. L. Willis, M. D. Trombley, C.-H. Chen and C. Proulx, *J. Am. Chem. Soc.*, 2025, **147**, 1404–1410.

10 For C–N and C–C atropisomeric peptidomimetics, see: (*a*) N. J. Roper, A. D. G. Campbell, P. G. Waddell, A. K. Brown, K. Ermanis and R. J. Armstrong, *Chem. Sci.*, 2024, **15**, 16743–16751; (*b*) B. Paul, G. L. Butterfoss, M. G. Boswell, P. D. Renfrew, F. G. Yeung, N. H. Shah, C. Wolf, R. Bonneau and K. Kirshenbaum, *J. Am. Chem. Soc.*, 2011, **133**, 10910–10919; (*c*) B. Paul, G. L. Butterfoss, M. G. Boswell, M. L. Huang, R. Bonneau, C. Wolf and K. Kirshenbaum, *Org. Lett.*, 2012, **14**, 926–929; (*d*) Y.-J. Wu, P.-P. Xie, G. Zhou, Q.-J. Yao, X. Hong and B.-F. Shi, *Chem. Sci.*, 2021, **12**, 9391–9397; (*e*) Z.-S. Jia, Y.-J. Wu, Q.-J. Yao, X.-T. Xu, K. Zhang and B.-F. Shi, *Org. Lett.*, 2022, **24**, 304–308; (*f*) I. J. Knudson, T. L. Dover, D. A. Dilworth, C. Paloutzian, O. Paz, J. Lin, H. Cho, T. Gonen, A. Schepartz and S. J. Miller, *Nat. Chem.*, 2025, DOI: **10.1038/s41557-025-01935-4**; (*g*) T.-Y. Jiang, Y.-T. Ke, Y.-J. Wu, Q.-J. Yao and B.-F. Shi, *Chem. Commun.*, 2023, **59**, 13518–13521; (*h*) M. C. Morejón, A. Laub, B. Westermann, D. G. Rivera and L. A. Wessjohann, *Org. Lett.*, 2016, **18**, 4096–4099; (*i*) P. W. Glunz, L. Mueller, D. L. Cheney, V. Ladziata, Y. Zou, N. R. Wurtz, A. Wei, P. C. Wong, R. R. Wexler and E. S. Priestley, *J. Med. Chem.*, 2016, **59**, 4007–4018; (*j*) N. K. Mothahalli Raju, B. Paul, L. TN, S. Bodduna and N. K. Kandukuri, *J. Org. Chem.*, 2025, **90**, 4796–4807.

11 J.-P. Heeb, J. Clayden, M. D. Smith and R. J. Armstrong, *Nat. Protoc.*, 2023, **18**, 2745–2771.

12 A. D. G. Campbell, N. J. Roper, P. G. Waddell, C. Wills, C. M. Dixon, R. M. Denton, K. Ermanis and R. J. Armstrong, *Chem. Commun.*, 2024, **60**, 3818–3821.

13 (*a*) CCDC 2476444: Experimental Crystal Structure Determination, 2025, DOI: **10.5517/ccdc.csd.cc2p3y92**; (*b*) CCDC 2476445: Experimental Crystal Structure Determination, 2025, DOI: **10.5517/ccdc.csd.cc2p3yb3**.